RESEARCH

Submerged reef features in Apo and Tubbataha Reefs, Philippines, revealed paleo sea-level history during the last deglaciation

Jeffrey C. Munar[1,2] · Mario A. Aurelio[2] · Edwin E. Dumalagan Jr[1] · Erin Joy C. Tinacba[1] ·
Ma. Angelique A. Doctor[1] · Fernando P. Siringan[1]

Abstract
The morphology of coral reefs provides an effective benchmark of past sea levels because of their limited vertical range of formation and good geologic preservation. In this study, we analyze the seafloor morphology around two atolls in the Philippines: Tubbataha Reef, in Palawan, and Apo Reef, in Occidental Mindoro. High-resolution multibeam bathymetry to a depth of 200 m reveals seafloor features including reef ridges and staircase-like terraces and scarps. Depth profiles across the reefs show terraces formed within six and seven depth ranges in Tubbataha Reef and in Apo Reef, respectively. These were further observed through a remotely operated vehicle. The terraces and scarps are interpreted as backstepping reefs that were drowned during an overall rise in sea level from the Last Glacial Maximum (LGM). Terraces are used as indicators of paleo sea level and the separation between terraces as the magnitude of sea-level rises coeval with meltwater pulse events during the last deglaciation. The pattern for both Apo and Tubbataha reefs indicates subsidence, consistent with the absence of Holocene emergent features and their atoll morphologies. Subsidence of up to 17 m since the LGM in Apo Reef is mainly attributed to the downbowing of the crust toward Manila Trench. In Tubbataha Reef, subsidence of up to 14 m is attributed to the continuous cooling of the volcanic crust underlying the atoll. These can be used to fill gaps in the tectonic history of the study sites from the last deglaciation.

Introduction

Coral reefs are the largest biologically constructed features on the seafloor and are characterized by their complex structure and ecology (Wood 1999). Their morphologies provide significant evidence for past sea levels due to their limited vertical range, high potential for preservation, and suitability for dating (Lighty et al. 1982; Stoddart 1990; Woodroffe 2008; Woodroffe & Webster 2014). Reef morphology is a product of changing sea levels as well as the physical and ecological conditions during its formation (Lutzenkirchen et al. 2023, Montaggioni 2005; Smith and Buddemeier; 1992; Stoddart; 1969; Woodroffe and Webster 2014).

Models by Neumann and Macintyre (1985) and Davies and Montaggioni (1985) outline how reef growth responds to the availability of accommodation space and can be altered by sea-level fluctuations. Reefs may be able to vertically "keep up" if accretion rates are roughly equal to the rate of sea-level rise. Reefs may not initially keep pace with sea-level rise, but deep reef communities can be progressively replaced by shallow water forms and "catch up" with sea level. Reefs drown when reef accretion is inhibited as it significantly lags with the rise of sea level (Blanchon and Shaw 1995) and backstep when there is an available landward substrate behind to retreat into (Hubbard et al. 1997). Reefs emerge when relative sea level drops, exposing reef sections to the surface (Dickinson 2001). During prolonged sea-level stability, shallow reefs are forced to grow horizontally toward the available seaward space. Extensive horizontal reef surfaces provide vertical reference points for the upper growth limit of coral reefs during this period (Kennedy and Woodroffe 2002; Montaggioni 2005). Antecedent substrates and exposed reefs are subject to erosion by wave action (Grigg et al. 2002). This mechanism etches wave-cut platforms and marine notches close to sea level and produces

---

Communicated by Gabriele Uenzelmann-Neben.

✉ Jeffrey C. Munar
  jcmunar@msi.upd.edu.ph

[1] Marine Science Institute, University of the Philippines, 1101 Diliman, Quezon City, Philippines

[2] National Institute of Geological Sciences, University of the Philippines, 1101 Diliman, Quezon City, Philippines

a sea cliff landward (Kershaw and Guo 2001). Over time, multiple reef terraces indicate the number of interstadial sea-level events in a region (Woodroffe and Webster 2014). Combined with the vertical effect of tectonics, coral reefs are used to determine the relative sea-level (RSL) history (Woodroffe and Webster 2014).

Eustatic sea levels have risen by around 120 m since the Last Glacial Maximum (LGM) (Fairbanks 1989; Yokoyama et al. 2001; Hanebuth et al. 2000; Peltier 2002; Clark and Tarasov 2014; Austermann et al. 2013; Lambeck et al. 2014; Gowan et al. 2021). The rise of sea level has not been uniform, having episodes of relative stability during stillstands which are separated by rapid rises (Bard et al. 1996; Fairbanks 1989). Rapid rises in sea level are commonly attributed to meltwater pulses (MWP) associated with rapid ice melting or ice sheet collapses in high latitudes (Blanchon and Shaw 1995; Fairbanks et al. 1992; Harrison et al. 2019). During these pulses, sea levels have risen by as much as 60 mm/year based on submerged reef terraces and stacked delta records (Fairbanks 1989; Blanchon and Shaw 1995; Peltier 2002; Liu and Milliman 2004; Clark et al. 2004; Deschamps et al. 2012; Lin et al., 2021; Abdul et al. 2016; Harrison et al. 2019; Brendryen et al. 2020). In the Philippines, sea-level reconstructions during the Holocene are based on dated coastal reef terraces, mangrove deposits, tidal notches, and borehole data with age dates younger than 10.2 ka in Palawan, Bohol, Samar, and Ilocos (Berdin et al. 2003; Maeda et al. 2004; Omura et al. 2004; Ringor et al. 2004; Shen et al. 2010; Siringan et al. 2016). These records are based on emergent structures that reflect the Holocene sea-level highstand and uplift. Sea-level records in emergent reefs and tidal notches in northern Luzon and Palawan indicate three highstands (7.5–6.0 ka, 6.0–4.0 ka, and 2.8–1.2 ka) in the mid-Holocene some of which occur as high as 4.2 m (Maeda et al. 2009; Maeda and Siringan 2004). These deglacial sea-level trends were very similar to records from Abrolhos Island, Australia, and higher than the paleo sea-level records in Tahiti (Shen et al. 2010; Siringan et al. 2016). Higher than present paleo sea-level markers in Pangasinan, Davao, and Ilocos have also been attributed to co-seismic uplift events during the Holocene (Maxwell et al. 2018; Ramos et al. 2012; Ramos and Tsutsumi 2010). Reef terraces during the deglacial period up to a depth of 120 m were also mapped on Pag-asa Island (Janer et al. 2023). Higher than present paleo sea-level indicators towards 131 ka MIS-5e and 237 ka MIS-7 were also identified in Bohol and Palawan (Omura et al. 2004; Ringor et al. 2004).

The advent of high-resolution acoustic mapping allowed new insights into describing submerged reefs, which were formed during periods of lower than present sea level, at larger extents and high resolutions (Beaman et al. 2008; Grigg et al. 2002; Khanna et al. 2017). High-resolution multibeam echosounder surveys yield bathymetric data that can image fine-scale and laterally extensive morphological features on the seafloor including reef terraces (i.e., Abbey et al., 2011; Beaman et al. 2008; Conway et al. 2005; Gomes et al. 2020; Kan et al. 2015; Khanna et al. 2017; Kim et al. 2013; Lebrec et al. 2022; de Silveira et al. 2020; Storlazzi et al. 2003; Tibor et al. 2010; Varzi et al. 2023; Vieira et al. 2023; Zecchin et al., 2015). Past studies in Hawaii (Grigg et al. 2002), Maldives (Fürstenau et al. 2010; Rovere et al. 2018), Australia (Abbey et al. 2011; Beaman et al. 2008; Lebrec et al. 2022), Gulf of Mexico (Khanna et al. 2017), Mediterranean Sea (Zecchin et al. 2015), Ryukyus, Japan (Inoue and Arai 2020), Rio Grande do Norte, Brazil (Gomes et al. 2020), and Abrolhos Shelf, Brazil (Vieira et al. 2023), have shown that the morphology of submerged reef terraces can provide regional interpretation of the origins and development of reefs even in the absence of age-dated materials.

In this study, high-resolution multibeam echosounder data along with remotely operated vehicle observations were acquired along the upper slopes of Apo and Tubbataha Reef, in the Philippines, down to a depth of 200 m, to identify and describe submerged coral reef terraces and ridges. The study aims to identify and describe submerged features of coral reefs from the bathymetric data. This can give insights into how coral reefs in the archipelago have responded in the past and their resilience to future sea-level changes. Recognizing the nature of past sea-level rises during deglaciation is critical for informing predictions on the future vertical behavior of global oceans. This study can also be used to further understand the neotectonic movements of the study sites since the LGM.

Regional setting

Apo Reef (12.67° N, 120.46° E) is located in Mindoro Strait, about 40 km west of Mindoro Island, Philippines. On the other hand, Tubbataha Reef (8.89° N, 119.73° E) is located in the middle of the Sulu Sea, about 160 km southeast of Palawan Island, Philippines (Fig. 1). Regionally, both are located around the Palawan microcontinent (PMC), a margin of the Sundaland-Eurasia plate that converges toward the Philippine Sea Plate (PSP) (Aurelio 2000). PMC converges to the western side of the Philippine Mobile Belt, an active region that accommodates subduction from opposing polarities due to the convergence with PSP (Aurelio 2000) (Fig. 1).

Apo Reef

Apo Reef is an offshore atoll found off the western coast of Mindoro Island (Fig. 1). The main reef body rises from a depth greater than 1000 m (Glenn-Sullivan and Evans 2001). The atoll consists of two sub-triangular reefs, on the northern and southern atolls (Bacabac et al. 2023).
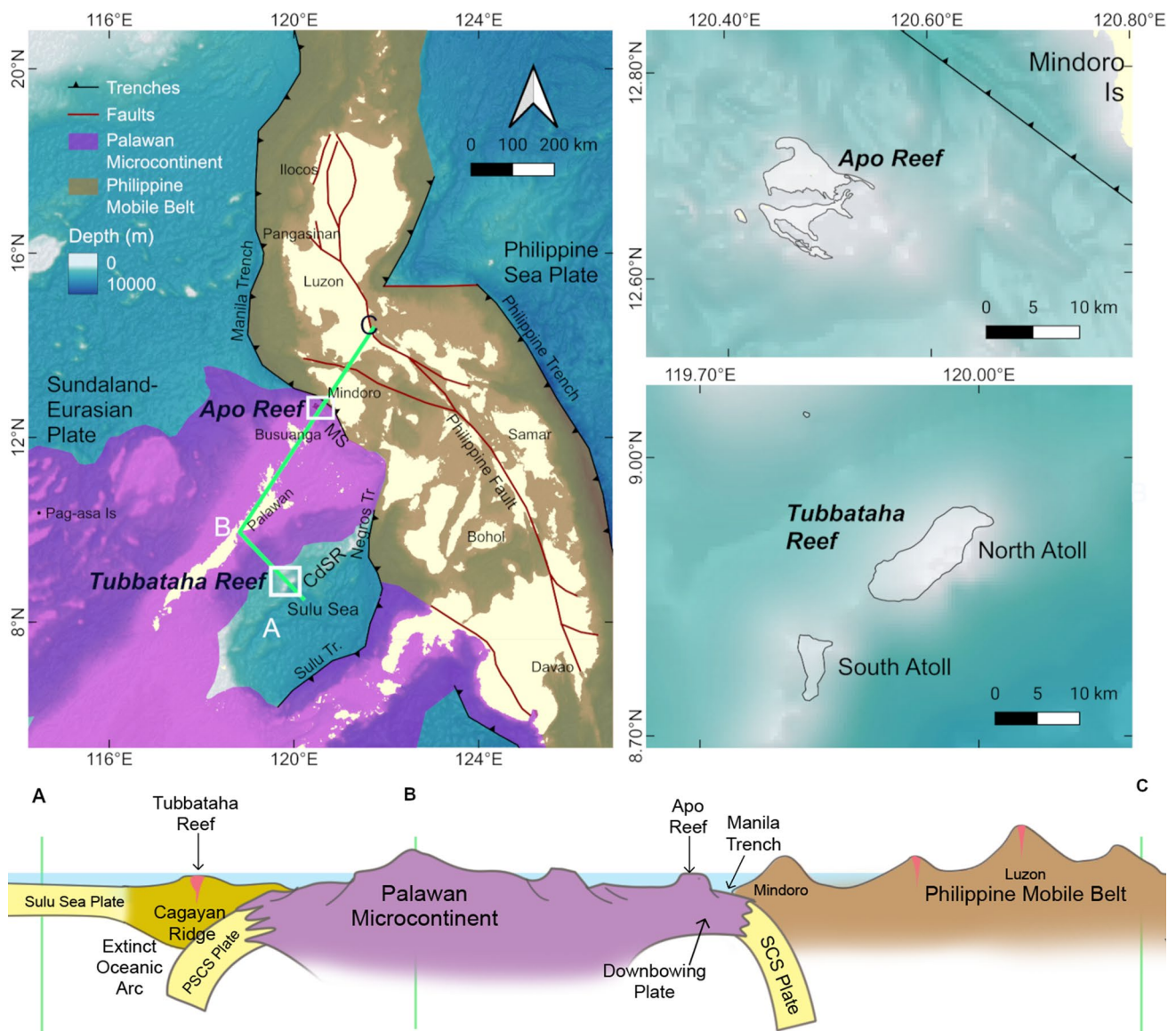
Fig. 1 Location of Apo Reef and Tubbataha Reef within the tectonic framework of the Philippines. Crustal boundaries are based on structural studies on the South China Sea and the Philippines by Aurelio et al. (2014), Franke et al. (2014), and Pubellier et al. (2018). The green line represents the position of the cross-section. (B) Schematic cross-section of the tectonic settings of Tubbataha Reef and Apo Reef. These were adapted from the studies by Hall et al. (1995), Li et al. (2014), Rangin et al. (1988), and Rangin and Silver (1991). Abbreviations: SCS = South China Sea plate, PSCS = proto-South China Sea plate, CdSR = Cagayan de Sulu Ridge, MS = Mindoro Strait

Apo Reef is built on a small submarine platform (Zacher 1981) within the Palawan-Reed Bank Continental platform, in the back-arc region of the southern end of Manila Trench. Manila Trench is an active east-dipping subduction zone that subducts the South China Sea plate toward Luzon Island (Aurelio 2000; Hayes and Lewis, 1984). The southern termination of the trench is characterized by a complex tectonic fabric formed between an arc-trench gap (Rangin et al. 1988). Onshore, north of Mindoro, is a transpressive region composed of parallel folds and thrust faults (Faure et al. 1989; Marchadier and Rangin 1990; Sarewitz and Karig 1986). Busuanga Island, on the south, is part of a stable continental fragment that has accreted since the Mesozoic (Zamoras and Matsuoka 2004). Offshore areas in North Palawan are underlain by the platform carbonates of Nido Limestone which started to formed during the Oligocene to Miocene (Steuer et al. 2013).

Apo Reef is located in the middle of Mindoro Strait, which connects the Sulu Sea and the South China Sea. The surface wind patterns in the study sites are impacted by the

East Asian Monsoon System (Pullen et al. 2011). In winter, they predominantly blow from the northeast, while in summer, they shift to southwesterly directions. During transitional periods, the wind patterns become highly unpredictable (Wyrtki, 1961). Mindoro Strait is predominated by a southward current that provides inflow to the Sulu Sea and is subject to anomalous northerly surges of reversals and cyclonic eddies during monsoon transitions (Hurlburt et al. 2011; Pullen et al. 2011).

Tubbataha Reef

Tubbataha Reef is an offshore atoll complex covering three reef atolls in the middle of the Sulu Sea (Fig. 1). The study site covers the north atoll of Tubbataha Reef. Two islets are located at the north (Bird Islet) and south (Ranger Station) ends of the north atoll (White and Palaganas 1991). Tubbataha Reef is among the reefs found on the southwest-northeast-oriented Cagayan Ridge across the Sulu Sea (Ledesma 2001).

Cagayan Ridge, also known as Cagayan de Sulu Ridge, is a remnant island arc associated with the ancient subduction of the proto-South China Sea along the Palawan Trough (Rangin et al. 1990). The onset of the volcanism started during the Oligocene-Early Miocene and ended during the Middle Miocene (Rangin and Silver 1991). The cessation of its volcanism is associated with the docking of the Palawan-Reed Continental Platform toward the Sulu Basin (Rangin and Silver 1991). Cagayan Ridge is capped by up to 400-m-thick coralgal reef deposits that have been deposited since the Middle Miocene (Kudrass et al. 1990; Rangin and Silver 1991). This observation alongside dredged coral samples in Sibutu Passage at more than 500 m depth indicates that the reefs along the Cagayan Ridge have undergone significant subsidence (Krause 1966). Surface currents in the Sulu Sea exhibit seasonal changes coinciding with the monsoon system. In summer, currents predominantly originate from the south, while during winter, they form counterclockwise gyres (Wang et al. 2006).

Methods

Multibeam echosounder survey

High-resolution bathymetry was collected using an R2Sonic 2022 multibeam echosounder system mounted on the side of an outrigger boat. Surveys on Apo Reef were conducted on May 27–29, 2015, and March 12–17, 2016, and those on Tubbataha Reef North Atoll (TRNA) on April 4 and 5, 2016. The multibeam echosounder system was set at a frequency between 200 and 400 kHz with a maximum swath coverage of 160°, with beam widths of $1° \times 1°$ at 400 kHz and $2° \times 2°$ at 200 kHz. A conductivity, temperature, and depth (CTD) profiler was deployed daily to determine the sound velocity change in the water column within the survey area covered. Surveys were done at a speed of 3–5 knots, following the isobath of each site. The minimum depth that was surveyed is at ~5 m to avoid possible damage to the survey boat, and thus, the modern reef flat was not covered. The maximum depth of the surveys was set at 200 m. A frequency of 400 kHz was used for depths of 0–100 m and 200 kHz for depths between 100 and 200 m. Raw bathymetric data were post-processed using HYPACK and HYSWEEP software. Instrument setup measurements, tide level corrections, and CTD profile corrections were integrated with the raw data during this process. Harmonic tides from WXTide32 during the period of the survey were incorporated in the correction. Tidal range from the closest tide stations in Apo Reef is at 1.03 m and Tubbataha is at 1.4 m (NAMRIA 2022). Total propagated uncertainty for vertical depth measurements was determined at 18 cm. Grid models were then generated using HYPACK CUBE (combined uncertainty and bathymetric estimator) filtering and gridding algorithm (Calder and Mayer 2003) at a nominal spacing of 5 m for interpretation of geomorphology and to account for GNSS positioning errors. Bathymetric data were gathered around each atoll in Apo Reef. The northeastern edge of the North Atoll was not surveyed due to poor accessibility from the base station on Apo Island. The channel separating the North Atoll and South Atoll was also covered. For Tubbataha Reef, sections within the west and east of the north atoll were covered. Covering the whole extent of TRNA was not possible due to time constraints.

Terraces were analyzed for their continuity by observing and manually tracing the change of curvature or slope breaks computed in the bathymetric data. This was done by inspecting corresponding bathymetry, slope, and curvature. Profiles were also extracted every 100 m in a downslope direction to aid in identifying terraces. Terrace values from the bathymetric profiles were measured at the base of the terrace. When the terrace base is not well defined, it is represented by the point where the curvature is at maximum value between the terrace and scarp. This ensures that the depth represents the least amount of vertical sedimentation. Terraces were also scrutinized for their continuity within the reef body. Hypsograms were computed from the gridded bathymetric data. Flatter reef surfaces are represented as peaks in the hypsogram that correspond to broad features in a reef. Terrace continuity and hypsograms were used to estimate the range of depths of each terrace (Harris et al. 2008). Depth ranges are determined by the minimum and maximum depth determined for each terrace. Descriptions of mapped reef features follow the definitions

of the International Hydrographic Organization for naming undersea features. Slopes were described in this paper using the following modifiers: flat (0–5°), gentle (5–30°), steep (30–60°), and sub-vertical (80–90°).

In the absence of age-dated materials, we use sea-level records from the West Pacific to reference the age of the submerged reef terraces. The derived terrace depths from the bathymetric data are compared to deglacial sea-level reconstructions from the Yellow River Delta (Liu et al. 2004) and Sunda Shelf (Hanebuth et al. 2011; Shaw et al. 2023). Yellow River Delta and Sunda Shelf sea-level records were gathered from transgressive sequences along passive margins. Coral reef records in the West Pacific were also included to reference reef formation during the last deglacial. This includes data from Tahiti (Bard et al. 1996) and Huon Peninsula (Ota and Chappell 1999). These records provide the most proximal and complete reconstructions of sea level in the past 19,000 years. Sea-level records in the Philippines that span the past 10.2 ka (Maeda et al. 2009, 2004; Shen et al. 2010; Siringan et al. 2016) provide information on higher than present sea-level stands.

Underwater camera observation

A remotely operated vehicle (ROV) was deployed to document the nature of the reef substrate. Action cameras were attached to the ROV to retrieve high-resolution images aside from the video footage from the ROV. The ROV was driven close to the corals, seafloor, walls, and other reef structures to allow identification of reef features. Video footages retrieved from the ROV and the action cameras were analyzed for the presence of corals and the character of the substrate. Three sites for ROV deployment were done in Apo Reef, and two sites were done for Tubbataha Reef (Table 1).

Table 1 Deployment sites for remotely operated vehicle (ROV) surveys

| Site	Location	Maximum depth surveyed
Apo Reef		
Apo Island	12.6530° N, 120.4199° E	149 m
North Atoll	12.7355° N, 120.4622° E	78 m
South Atoll	12.6352° N, 120.4549° E	80 m
Tubbataha Reef North Atoll		
East side (Malayan site)	8.8844° N, 119.8850° E	156 m
West side (shark point)	8.9345° N, 120.0081° E	120 m

Results

Apo Reef

Apo Reef is separated into three areas: Apo Reef North Atoll (ARNA), Apo Reef South Atoll (ARSA), and Apo Island (Fig. 2). Small coral limestone outcrops occur within the reefs: Cayos del Bajo (locally named Tinangkapan Island), a 100-m-wide outcropping rock within the ARNA, and Apo Menor Island (locally named Binanggaan Island), a 250-m-wide outcropping rock within the western portion of the South Atoll. To the west, Apo Island is a separate structure, wherein a 500 m sandy beach has accumulated around a limestone outcrop (Fig. 3). The surfaces of the limestones are highly karstified. Limestone exposures are observed as massive, gray-white, non-porous, and crystalline. These limestone outcrops are well cemented and indurated. Tidal notches above present levels are also absent in the outcrops.

Figure 2 shows the distribution and horizontal continuity of the terrace edges traced from the bathymetric model. The morphology of each reef varies. Both the ARNA and Apo Island have very predominantly steep slopes around them (Fig. 4). In contrast, the South Atoll has a gentle slope on its southeastern side. Notably, the rims of all three reefs have multiple, continuous paired terraces and scarps. The depths covered by the terraces are summarized in Table 2.

Apo Island

Four continuous terraces were mapped around Apo Island. Terraces at the northwest and southeast sides are wider. The shallowest surveyed terraces on Apo Island occur at A1, 7 ± 1 m, and A2, 14.5 ± 3.5 (Fig. 5). Spur and groove structures on the island are closely spaced and typically over a 100 m long, running obliquely around the island and terminate below A1. The upper reef terraces at A1 are dominated by branching and tabulate *Acropora*, with a few columnar and encrusting corals and crinoids. The gentle drop-off is covered by similar branching and tabulate corals. The rubble-filled ledges are mostly tabulate and encrusting coral colonies and a few branching *Acropora*. Dense and diverse clusters of tabulate and encrusting *Acropora*-dominated wall line beyond A1. Although the rocky wall is steep, its surface was also quite complex with ledges, large crevices, and overhangs built from dead corals and colonized by gorgonians, soft corals, and crinoids. Spur and groove structures are observed in the shallowest reef terrace of Apo Reef extending up to a depth of 18 m at the base of A2. A2 is dominated by branching and tabulate

Fig. 2 A Relief chart of the bathymetry around Apo Reef, Occidental Mindoro based from multibeam echosounder surveys. White boxes indicate the extent of three-dimensional renders from (B)–(D). Points indicate locations where the ROV is deployed. Three-dimensional renders of the bathymetric features in Apo Reef in **B** North Atoll, **C** within the depression between the North Atoll and South Atoll, **D** Apo Island, and **E** South Atoll. Reef terraces with their outer edges are outlined by white dashed lines; reef ridges are outlined by black dashed lines. Vertical exaggeration at ×1.5
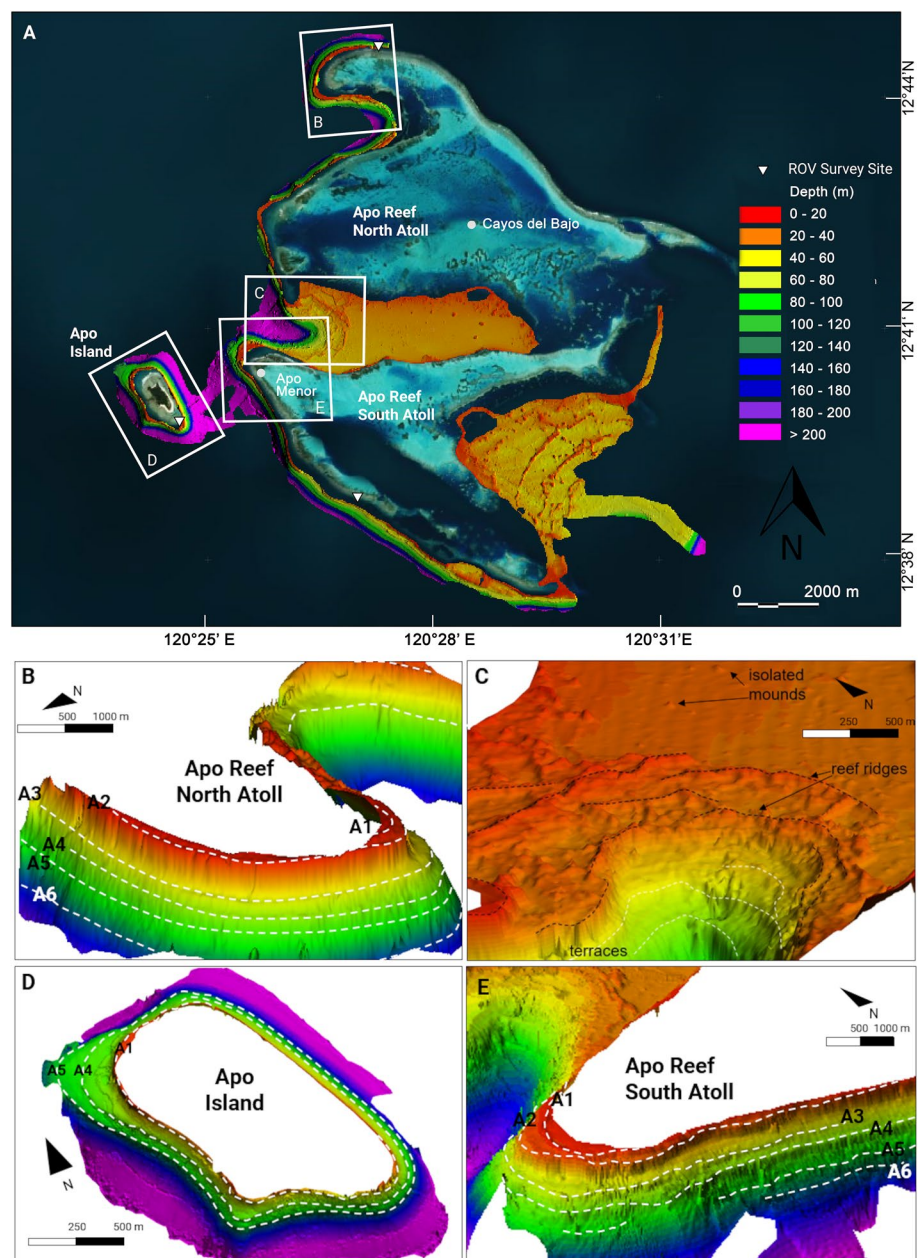
Acropora, with a few encrusting corals. Clusters of small and large sea fans, hydroids, and diverse sponges were seen interspersed with encrusting and a few plating corals such as *Mycedium*.

The wall from 58 m depth and deeper is covered in sand and rubble until the slope is interrupted by the terrace at A4, 74 ± 6 m. The terrace at A4 and its scree-buttress slope have patches of rocks that extend down to the lower mesophotic depths. Hydroids, sponges, soft corals, sea fans, and other gorgonians were found on top of dead corals at this depth. The wall beyond A5, 102 ± 7 m, had no lifeforms except crinoids (at 143 m) up to 149 m, and the maximum depth reached by the ROV. It should be noted

that A3 terrace, present from the rest of the reef, is absent in Apo Island and may have been poorly formed within its slopes.

Apo Reef North Atoll

Eight terraces were mapped around ARNA. The northwest wall and the more protected areas of the reef area are wider as compared to its west wall. Terraces at the northwest wall are 47% wider than the rest of ARNA.

The shallowest sets of surveyed terraces occur at A1, 6.5 ± 0.5, and A2, 20.5 ± 0.5. The reef terraces at A1 and A2 are dominated by tabulate *Acropora* (Fig. 6). Beyond

Fig. 3 Surface features around Apo Reef include: Apo Island (**A**) is a sand shoal that has grown around rock outcrops similar to (**B**) Apo Menor Island. Surface features in Tubbataha Reef are sand shoals like the Ranger Station (**C**) and small protruding rocks (**D**) around Bird Islet
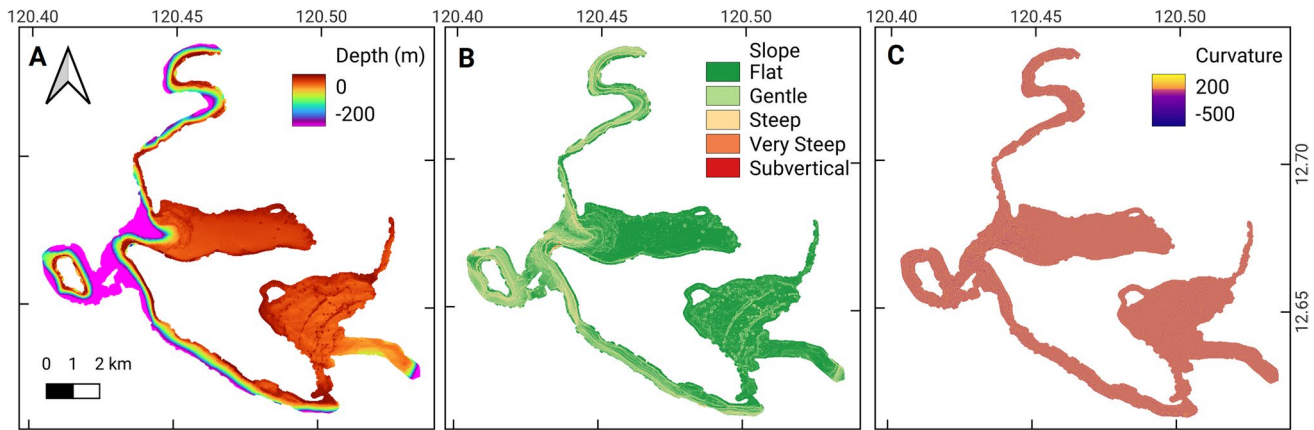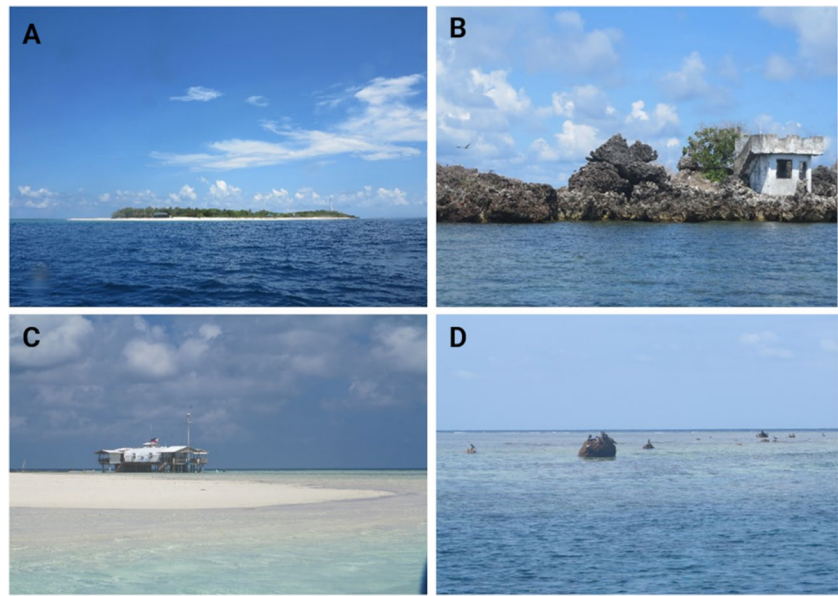

Fig. 4 **A** Bathymetry, **B** slope, and **C** curvature map of the seafloor around Apo Reef

Table 2 Summary of the depth ranges of terraces around Apo Reef, Occidental Mindoro, and Tubbataha Reef, Palawan derived from collected bathymetric data

Measured terrace depth (RTd) $\pm$ σRTd (m)

	Apo Island	Apo Reef North Atoll	Apo Reef South Atoll		Tubbataha Reef
A1	7 ± 1	6.5 ± 0.5	9 ± 5	T1	7 ± 1
A2	14.5 ± 3.5	20.5 ± 0.5	26 ± 4	T2	19 ± 5
A3	–	62 ± 2	48 ± 3	T3	70.5 ± 4.5
A4	74 ± 6	76 ± 2	76 ± 4	T4	92 ± 4
A5	102 ± 7	92 ± 1, 106. 5 ± 3.5	103 ± 8	T5	116 ± 6
A6	–	151 ± 5	137 ± 2	T6	134 ± 2
A7	–	189 ± 5	–		

A2, the steep upper drop-off or wall has a diverse assemblage of tabulate and branching *Acropora*, as well as *Seriatopora*, *Millepora*, flat sponges, gorgonians, and encrusting *Porites*, among others. From the drop-off to a reef wall from A2, there is a decreasing cover of branching corals and an increasing cover of sea fans, other gorgonians, hydroids, flat sponges, vase sponges, barrel sponges, and encrusting corals. At depth, the terraces occur between A3, 62 ± 2 m; A4, 76 ± 2 m; A5a, 92 ± 1 m; A5b, 106. 5 ± 3.5 m; A6, 151 ± 5 m; and A7: 189 ± 5 m (Fig. 5). Within A3 terrace, the seabed is covered by sand, rubbles, and dead corals, which are colonized by gorgonians. At 78 m, within A4, the maximum depth reached by the ROV, is a large sandy and rubbly area with few patches of gorgonians.
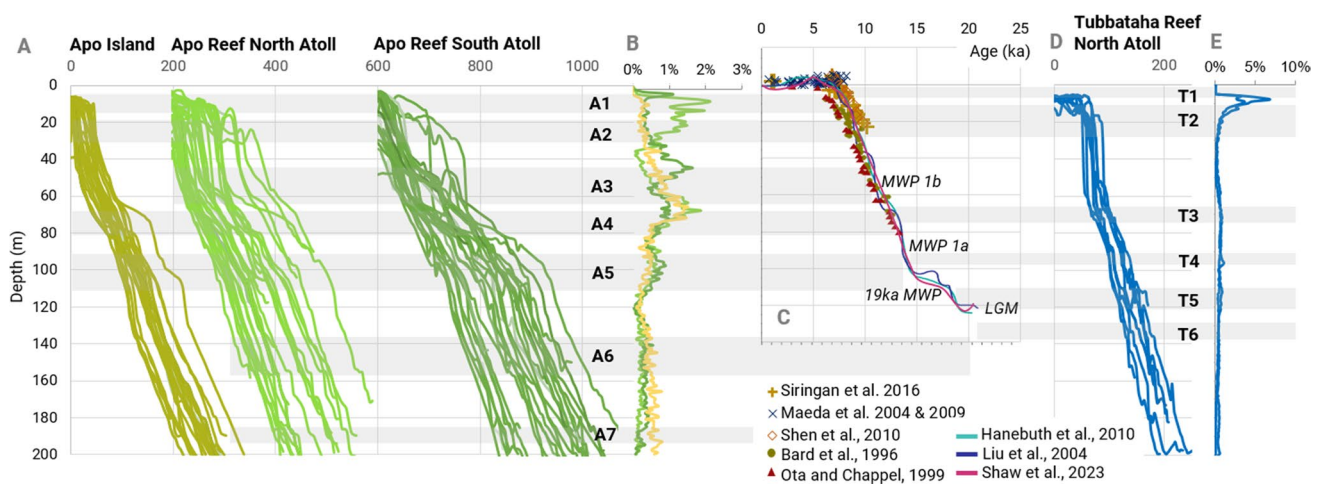
Fig. 5 Stacked profiles generated from the bathymetric data across each area in Apo Reef (**A**) and hypsometric curve showing the distribution of depths in Apo Reef (**B**). **D** Stacked profiles generated from the bathymetric data from Tubbataha Reef along with **E** hypsometric curve of the data. The vertical extent of the gray bars indicated the depth range of each terrace. These ranges are compared to the reconstructed paleo sea levels in the West Pacific region (**C**)

Apo Reef South Atoll

Six terraces were mapped around ARSA. The west side has distinct sub-vertical slopes between 30 and 72 m. In contrast, ARSA has gentle slopes toward its southeastern margin. Terraces found facing southeast are 17% wider than the rest of the reef.

The shallowest terrace in South Atoll is A1 at 9 ± 5 m. The reef within A1 is mostly composed of tabulate *Acropora*, branching corals, and massive *Porites* (Fig. 6). The forereef slope starting beyond A1 has among the most diverse, extensive, and contiguous live coral coverage seen in Apo Reef. A1 terrace then gradually transitions to a deeper terrace A2 at 26 ± 4 m. Approaching A2 terrace, tabulate and branching *Acropora*, other branching corals, and foliose corals are interspersed with soft corals, but foliose corals of *Montipora* start to dominate. The steep slope area beyond A2 has foliose corals along with a few hydroids and gorgonians. The reef then drops into a steep wall which is broken by the terrace at A3, 48 ± 3 m. A3 terrace contains plating and encrusting corals, including *Porites*, and dead corals colonized by large sea fans, whip corals, and crinoids. Beyond A3, the rocky wall was colonized by large sea fans and gorgonians. The wall beyond A3 toward A4, 76 ± 4 m, is covered mostly by sand and rubbles, with some relatively flat, rocky patches colonized by sea fans, whip corals, and crinoids. Smaller terraces were also identified at A5, 103 ± 8 m, and A6, 137 ± 2 m, within the reef wall (Fig. 5).

An east–west-oriented depression ranging from 20 to 49 m deep separates the ARNA and ARSA (Fig. 2C). This depression is deeper toward the West. Several discrete reef mounds with heights of 2 to 15 m are scattered within this area. Ridges occur within the west side of this depression and in the southwest portion of the atoll. These ridges rise about 10 m from the seafloor from the edge of terraces that are shallower than 30 m. The tops of the ridges are bimodal with peaks at depths of 14 m and 28 m. At least five sets of ridges are found to run subparallel to each other (Fig. 2C).

Tubbataha Reef North Atoll

Tubbataha Reef North Atoll (TRNA) rises from depths of 500 m and is elongated NE-SW following the trend of the Cagayan Ridge. The shape is typical of an atoll with a shallow reef crest which rises close to the surface and a 40-m-deep lagoon (Dygico et al. 2013). Shallow sand bars are found in the northeast and southern regions of the reef, on Bird Islet and Ranger Station respectively (Figs. 7 and 8).

Terrace morphology observed on TRNA

Five terraces were identified from the bathymetric data of TRNA. The shallowest mapped terrace of TRNA, T1, is at 7 ± 1 m (Fig. 5). Terraces in the eastern section are wider by 26% compared to the west. ROV coverages in TRNA show that branching *Acropora* are dominant in the upper 8 m (Fig. 9). *Porites*, *Millepora*, *Heliopora*, *Favites*, *Goniopora*, and *Leptoria* are also identified within T1. The shallow area is interspersed with sandy regions containing coral rubbles.

The expansive shallow T1 terrace then breaks to the deeper T2 terrace at 19 ± 5 m. Tabulate *Acropora* and plating *Porites rus* are predominant within T2. Other identified corals are plating forms of *Montipora*, *Echinophyllia*, and *Pachyseris*. Coral heads of *Fungia*, *Lobophyllia*,
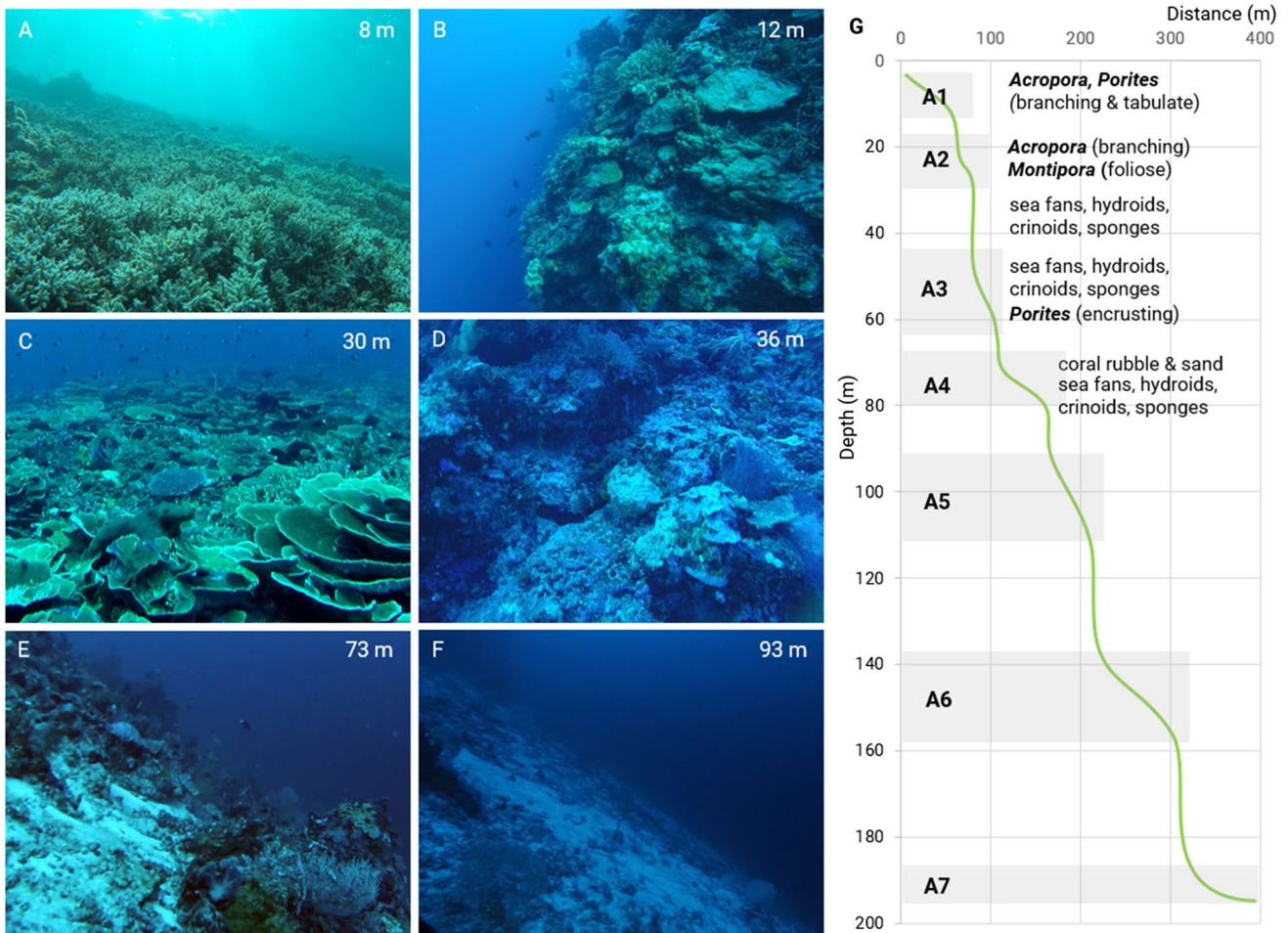
Fig. 6 Photographs from the ROV deployment show the composition of the seabed at different depths in Apo Reef. **A** Shallowest terrace within A1 at 8 m dominated by branching *Acropora*; **B** reef wall at 12 m covered by scleractinian corals *Acropora* and *Porites*; **C** terrace within A2 at 30 m dominated by foliose *Montipora*; **D** reef wall at 36 m containing encrusting corals, hydroids, and sponges; **E** terrace at A4 at 73 m covered mostly by sand and rubbles with few mesophotic communities of sea fans and hydroids; and **F** terrace at A5 93 m, covered mostly by sand and rubbles with few sea fans. **G** Schematic cross-section of the depth profile in Apo Reef and the dominant composition of coral genera and seabed material per depth based on ROV observations

and *Symphillia* were also identified. Beyond T2, the slope becomes sub-vertical. This also marks the base of spur and groove structures within the reef. Hard corals only occur within a reef wall until 36 m. These include *Diploastrea*, *Porites*, *Pachyseris*, *Oxypora*, and *Leptoseris*. Beyond 36 m, sea fans, soft corals, and sponges are usually seen along the reef slope and terminations of the terraces.

The steep slope of the reef wall is broken by smaller terraces T3 at 70.5 ± 4.5 m, T4 at 92 ± 4, T5 at 116 ± 6 m, and T6 at 134 ± 2 m. Terraces T3 to T6 are not as defined as T1 and T2 due to the steepness of the slope (Fig. 8). Reef walls are of bare carbonate rock, while coral rubbles and sand dominate the gentler regions of the seafloor. Few sea fans and sponges are identified in these depths. ROV observations reached a maximum depth of 156 m on a barren rocky slope within the east side of the reef.

Discussion

Formation and sea-level history

The rise of sea level since the LGM with intervening episodes of relative stillstand is considered the main driver for the staircase-like morphology of the reef terraces in Apo Reef and TRNA. A pair of terraces and scarp is interpreted as the former coral reef flat and reef front, respectively. The series of terraces were formed through subsequent backstepping during rapid rises of sea level and eventual re-establishment and progradation in a higher position during stillstands. The terraces then are taken as having formed during a relative sea-level stability while the scarp height approximates the magnitude of sea-level change.
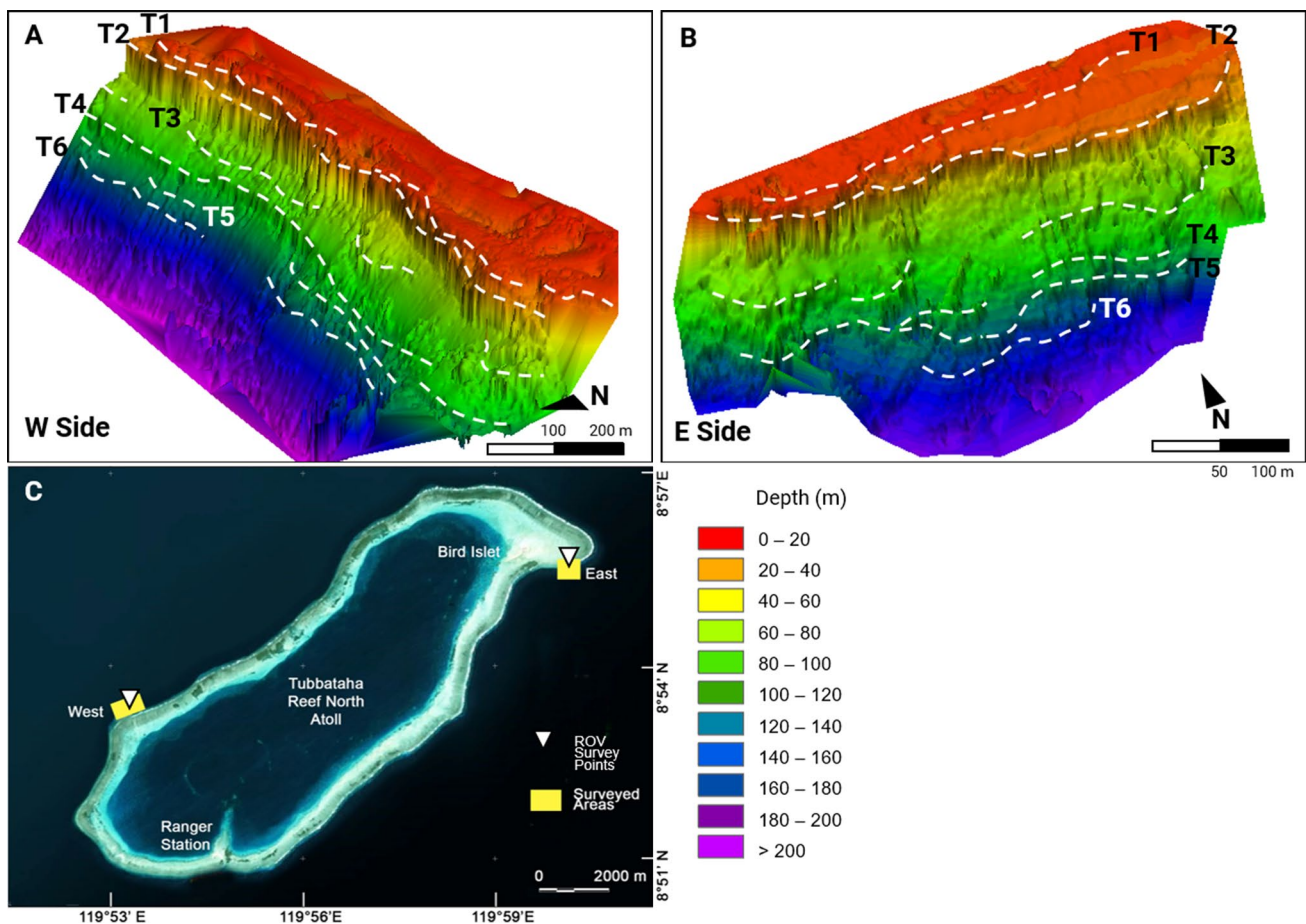
Fig. 7 Three-dimensional renders of the bathymetry in Tubbataha Reef on the west section (**A**) and east section (**B**) show reef terraces with their outer edges outlined by white dashed lines. **C** Location of survey sites in Tubbataha Reef North Atoll. Yellow boxes represent areas surveyed by multibeam echosounder surveys. Points indicate locations where the ROV is deployed

Highly variable vertical accretion rates were observed in the Indo-Pacific region from 1 to 30 m/ky and averaging at 6–7 m/ky in framework-dominated reefs (Montaggioni 2005). Indo-Pacific reefs develop with lower vertical accretion rates at an average of 4.4 m/ky compared to Caribbean reefs which grow at an average of 6 m/ky (Dullo 2005). Within the Philippines, faster accretion rates were recorded in Currimao, Ilocos Norte at 10 to 13 m/ky (Shen et al. 2010). Due to this variability, reefs can easily keep up with small sea-level perturbations. Furthermore, the data of Shen et al. (2010) and Janer et al. (2023) for the coral reefs in Currimao and Pag-asa Island, respectively, provide very fast rates of coral reef progradation. Borehole data in Currimao indicate progradation that can reach 75 m/ky (Shen et al. 2010). The morphology of reef terraces in Pag-asa Is. provides an estimate of the progradation rate that exceeds 150 m/ky (Janer et al. 2023). The width of the terraces also provides indications of the duration of relative sea-level stability and the influence of oceanographic factors that contributed to their development.

Table 2 summarizes the measured range of terrace depths at both sites. Within the last 19,000 years in the West Pacific, the most widely recorded meltwater pulses include post-19 ka MWP, MWP-1a, and MWP-1b. Post-19 ka MWP is known as a rapid rise from 120 m following the Last Glacial Maximum (Clark and Mix 2002; Yokoyama et al. 2001). Records from Bonaparte Gulf, Australia, indicate a 10–15 m rise in sea level from the LGM (Clark et al. 2004). MWP-1a involves a 17.9 m jump in sea level from 14.65 ka (Brendryen et al. 2020; Lin et al. 2021; Weaver et al. 2003). The depth of this jump in sea level ranges from 80 to 96 m (Hanebuth et al. 2000, 2011) and 80 to 95 m (Liu et al. 2004). The younger and shallower MWP-1b is an 8–11 m rise in sea level that occurred after 11.5 ka (Abdul et al. 2016; Bastos et al. 2022; Blanchon et al. 2021; Harrison et al. 2019; Tian et al. 2020). The extensive terraces at A6 to A3 in Apo Reef and T6 to T3 in TRNA (Fig. 5) are potential records of reef establishment around the events of 19 ka MWP, MWP-1a, and MWP-1b. In particular, terraces A3 and T3 are coeval with the records from the Sulu
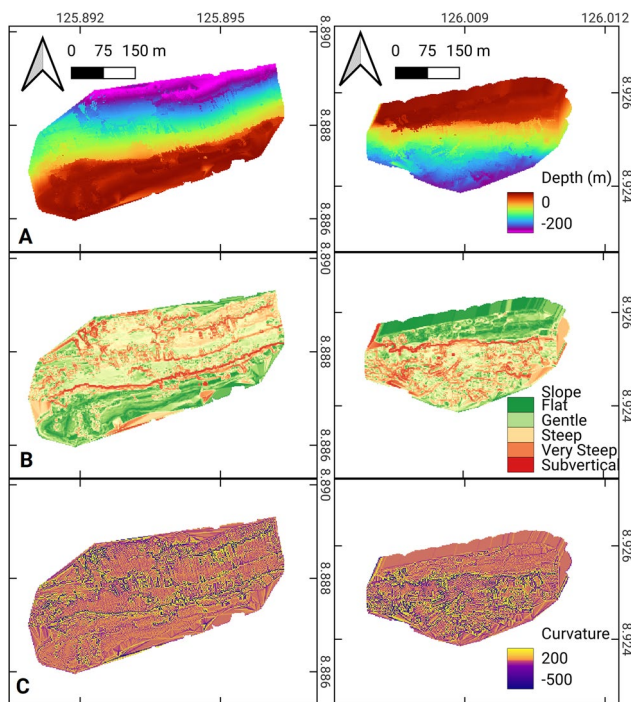
Fig. 8 **A** Bathymetry, **B** slope, and **C** curvature map of the seafloor within the surveyed sections in Tubbataha Reef

Sea during the Younger Dryas preceding the sea-level rise during MWP-1b (Linsley and Thunell 1990). During this period, oxygen isotope records indicate that the Sulu Sea experienced lower sea surface temperatures and lower salinity due to increased riverine discharge (Linsley and Thunell 1990). Such conditions contribute to slower reef growth during the formation of terraces A3 and T3.

The terraces at A1 and T1 are interpreted to have formed within the 6–7 ka highstand observed at 0.3–1.5 m in Palawan Island by Maeda et al. (2004). Holocene records likely kept pace with vertical accretion after the mid-Holocene highstand. These comprise the shallowest reef in both sites and are also associated with the modern shallowest reefs in the region. Both Apo Reef and TRNA have no marine terraces higher than the present Holocene paleo sea levels. The emergent limestone outcrops in Apo Reef are well cemented and lithified. These outcrops are unlike the observed emergent Holocene reefs in the Philippines which commonly are fissile and porous with visible bioclasts (Gong et al. 2017; Shen et al. 2010). There are also no tidal notches above present sea levels around these limestone outcrops. In TRNA, the only emergent features are sandy shoals and coral boulders. The absence of indicators of higher than present Holocene paleo sea levels suggests that Apo Reef and TRNA are undergoing subsidence and are consistent with their atoll morphologies. This subsidence also allowed for vertical space for accommodating the growth of the shallowest modern reefs.

Alternatively, former coral reef deposits may have undergone marine terrace formation during relative stillstands forming a terrace on the seaward side and a scarp on the landward side (Kershaw and Guo 2001). The terraces and scarps can also be inherited topography from the existing carbonate platform that was formed pre-LGM. However, a post-LGM origin is favored because of the well-developed extant reefs which indicate rapid coral growth in the two study sites. Reef development from MIS 5e to MIS 2 is expected to occur in an irregular manner due to the general pattern of declining sea levels interrupted by brief but temporary rises in sea level (Waelbroeck et al. 2002). It is expected that with the sub-aerial exposure of much older terraces, they would be discontinuous. The traced terraces, though, show continuity throughout the reefs. Short-lived transgressions, coupled with wave erosion during subsequent sea-level declines, result in minimal to no suitable surfaces for the establishment of future reef growth (Pastier et al. 2019).

The depth approximation in this study should be noted as simplistic. Discerning the precise timing for the formation of the terraces based solely on reef morphology has inherent uncertainties. Using geomorphic indicators for sea level is dependent on the tidal range of the sites (Horton et al. 2018). Attenuating growth of coral reefs with depth also poses compounding uncertainties, with the uppermost terraces T1 and A1 likely accreting at the present time. The terraces are also subject to bioconstruction and deposition of rubble material closer to the toes of slopes. With these in mind, these interpretations should be viewed from a larger perspective with meter-scale approximations for the described events. Control on the timing of growth of the terraces should be considered for future studies by collecting samples through the reef.

Factors affecting reef growth

Antecedent topography is a primary determinant for growth patterns of modern reefs (Dechnik et al., 2015, Salas-Saavedra et al. 2018). Steep slopes inhibit progradation and result in more discreet reef features (Grigg et al. 2002; Woodroffe and Webster 2014). The presence of small, outcropping karstic rocks on Apo Reef provides evidence for an antecedent foundation for modern reef growth. These outcrops are related to the offshore platform carbonates of Nido Limestone which are mapped extensively north of Palawan and have the shallowest seismic records in the area of Apo Reef (Franke et al. 2014; Steuer et al. 2013). The base of Nido Limestone is dated Late Oligocene to Early Miocene and is coeval with the onshore units of St. Paul Limestone (Saldivar-Sali et al. 1981; Steuer et al. 2013). Antecedent topography also explains its irregular shape and separation of reef components and the relatively gentle slopes around
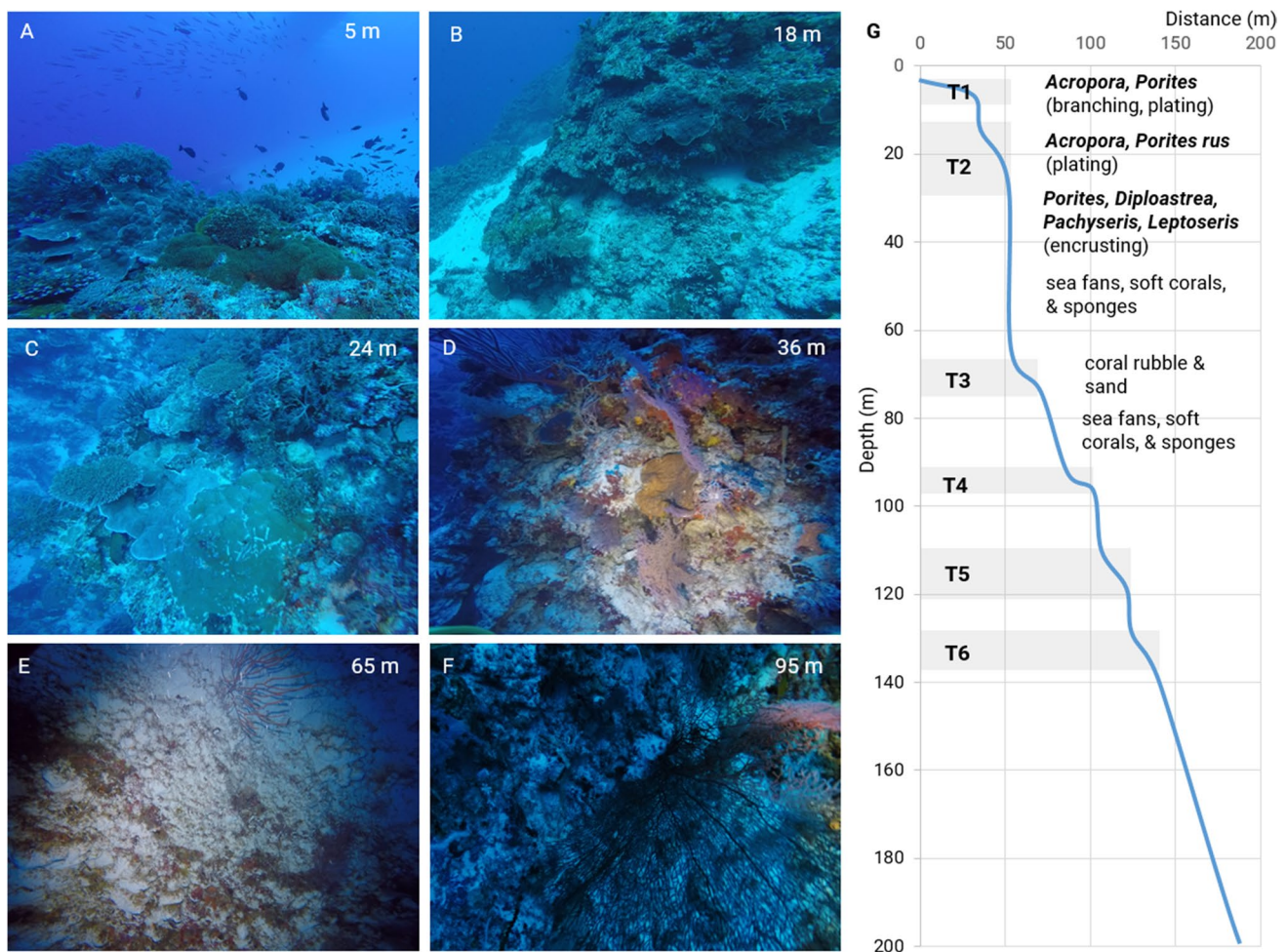
Fig. 9 Photographs from the ROV deployment show the composition of the seabed at different depths in TRNA. **A** Shallowest terrace within T1 at 5 m dominated by branching *Acropora* and *Porites*; **B** edge of the T2 terrace at 18 m with identified plating *Porites rus*; **C** terrace within T2 at 24 m covered by tabulate *Acropora*, and plating *Porites* and *Fungia*; **D** reef wall at 36 m containing encrusting *Lep-* *toseris*, sea fans, hydroids, and sponges; **E** reef wall at 65 m containing bare rock and sand along with some sea fans and sponges; and **F** terrace T4 at 95 m is covered mostly by sand and rubbles with few sea fans. **G** Schematic cross-section of the depth profile in TRNA and the dominant composition of coral genera and seabed material per depth based on ROV observations

the southeastern area of the reef. Steep slopes and antecedent topography are the primary limitations for reef progradation in TRNA, and as a result, only the shallowest platform becomes extensive. Combined with unrestricted vertical reef build-up, this resulted in the steeper slopes around TRNA.

Wave energy surrounding a reef also determines the growth pattern of a reef platform. Reef growth is faster in windward reefs than in leeward reefs because exposure to wave energy optimizes mixing and nutrient uptake (Hongo & Kayanne 2009). However, stronger waves such as large oceanic swells and storm currents can cause high mortality and erosion of reef-building corals, therefore inhibiting reef growth (Grossman & Fletcher, 2004). The unique position of the Apo Reef in Mindoro Strait exposes it to dynamic nutrient-rich currents that move between the

South China Sea and the Sulu Sea, predominantly toward the southeast direction (Pullen et al. 2011). Apo Reef is in a more open location from incoming southwest monsoons. Owing to more energetic waters, spurs and grooves are observed on the southwest side of Apo Island. Most well-formed terraces in Apo Reef are located in the more protected areas of the reef, away from the southwest, experiencing optimal wave energies for building up reefs. Being located in the middle of the Sulu Sea, TRNA is openly exposed to energetic waves and currents (Pullen et al. 2011). Dominant wind and wave patterns around TRNA are dictated by monsoons, with higher mean values coming from the southwest and northeast. This condition also contributes to the poor width of terraces in the surveyed areas.

Water clarity and temperature gradients of the oceans influence the depth limits of coral growth. High sedimentation rates generally have adverse effects on coral reefs and are associated with lower growth rates and reef demise (Kennedy and Woodroffe 2002; Perry et al. 2012; Webster et al. 2018). Oceanic reefs, like Apo and Tubbataha Reefs, are free from the effects of terrestrial sedimentation. The warm setting of the Sulu Sea and its surrounding waters also translate to warmer temperatures at depth (Gordon et al. 2011; Pullen et al. 2011). The depth limit of hard coral growth influences the extent to which reefs can grow to catch up with sea-level rise (Webster et al. 2018). Both Apo Reef and Tubbataha Reef have recorded hard corals that cover up to depths of 51 and 36 m, respectively. The presence of hard corals in these depths is indicative of the resilience of the reef to changes in sea level.

Reef crests, once submerged, develop into reef ridges (Grigg et al. 2002; Woodroffe and Webster 2014). In Apo Reef, these reef ridges are common within the depression that separates the atolls as well as the inner part of ARSA. These ridges represent the position of the reef crest that has constructively caught up with sea level (Woodroffe 2008). Alternatively, these are also parallel progradational ridges formed by the successive accumulation of coarse material during extreme wave events (Kench et al. 2022). This explains its formation within more sheltered areas of the reef. The distribution of these ridges in two depths at 14 m and 28 m indicates two periods of sea-level stability during its formation. These reef ridges may also be erosional (Grigg et al. 2002) but can only be confirmed if sampled or dated directly.

Departures from eustasy

The departure of the terrace depths from expected sea levels in the West Pacific considers two factors: glacio-isostatic adjustment (GIA) and tectonic motion. The study sites are located in a far-field region at the equator. GIA effects in the region account for a change of about −0.3 mm/year in the study area (Milne and Mitrovica 2008). This accounts for records of Holocene highstand at 2–3 m around Southeast Asia (Mann et al. 2019; Meltzner et al. 2017) during the past 6.5 ka BP (Li et al. 2023). Maeda et al. (2004) documented Holocene highstand tidal notches at 0.3–1.5 m above mean sea level in the central part of Palawan formed during around 6 ka BP. There are also records of undated emergent tidal notches found at 0.4–2.0 m above mean sea level along the coastlines of Sablayan and Sta. Teresa in Mindoro Island (Maeda and Siringan 2004). Existing nearby records indicate emergence, in contrast with the submergence in Apo Reef and Tubbataha Reef. This also implies that vertical motions in Apo Reef and Tubbataha Reef are separate from those

of the nearby Palawan and Mindoro Islands. Considering the extent of GIA influence and the compounding effect of subsidence, LGM is expected to occur below recorded levels in the West Pacific at 120 m (Clark and Tarasov 2014; Peltier 2002).

Apo Reef has a complex setting as it is located near the subduction zone of Manila Trench (Aurelio 2000). Two zones in this setting cause vertical changes: a zone of flexure experiences an overall uplift and a downbowing zone experiences subsidence (Fig. 10, Dickinson 2001). The limestones exposed in Apo Reef represent older carbonate platforms (Steuer et al. 2013), exposed during an earlier phase when Apo Reef reached the forebulge portion of the subducting slab. Apo Reef is only about 15 km from Manila Trench. This distance to the trench indicates that Apo Reef is now influenced by subsidence due to the downbowing of the subducting slab (Dickinson 2013). The subsidence of the crust is driven by discrete tectonic structures driven into the Manila Trench as it subducts under Mindoro Island (Rangin et al. 1988). The mismatch between the depth ranges of terraces between the three reefs in Apo Reef indicates varying magnitudes of vertical movement. The magnitude of subsidence in Apo Reef is estimated in two ways. On the shallowest mapped terrace, A1 at 9 m is the reef flat that formed during the 6.5 ka BP Holocene highstand. Using the depth difference from known records in this period, Apo Reef would have subsided by 10 m at a rate of 1.5 mm/year. This assumes that there is no accretion on the terrace after its formation. Alternatively, A6 terrace at 137 m corresponds to the terrace formed during the LGM which ended 19 ka. Given its depth difference with records of LGM levels, Apo Reef would have subsided by 17 m which would yield a rate of 0.9 mm/year. It is likely that subsidence in Apo Reef was not uniform or continuous through time given its location close to active tectonic structures (Chen et al. 2015; Rangin et al. 1988). Subsidence rates ranging between 0.9 and 1.5 mm/year are proposed for Apo Reef.

Tubbataha Reef sits atop an extinct volcanic arc that ceased volcanism during the Miocene (Fig. 10, Rangin and Silver 1991). The morphology of Tubbataha Reef is characteristic of a classic Darwinian atoll where the reef sits on a volcanic substrate. Vertical movement in this setting is caused by the thermal cooling of the lithosphere. The observed terraces are the latest formation in the continuing reef accretion on the extinct island arc of Cagayan Ridge. The shallowest terrace T1 at 6 m depth is formed during the 6.5 ka BP highstand. Given this difference with known records in this period, Tubbataha Reef would have undergone 7 m of subsidence or about 1 mm/year subsidence during 6.5 ka BP. Alternatively, the LGM depth of T6 at 134 m indicates that Tubbataha Reef, in the past 19 ka, would have subsided by 14 m or by 0.7 mm/year.
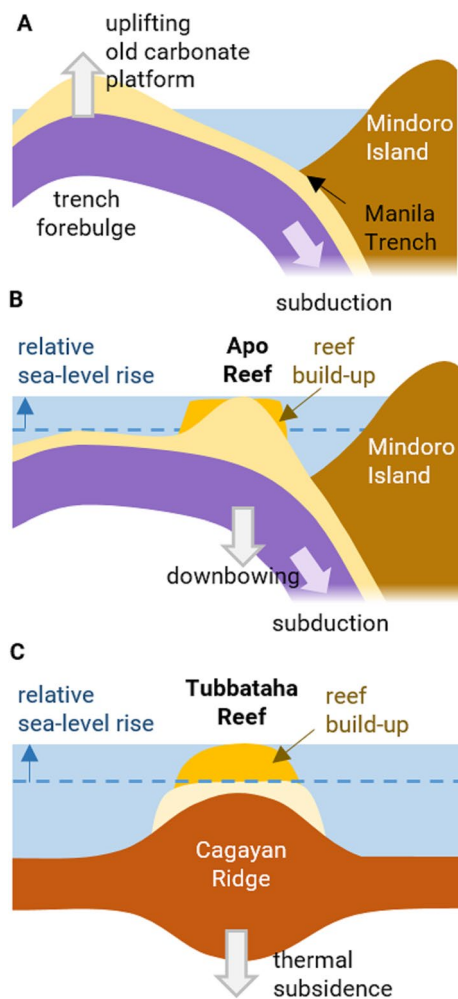
Fig. 10 Schematic diagram illustrating different tectonic influences on reef formation at the study sites: (**A**) old platform reefs located on the trench forebulge distal from Manila Trench (**B**) subsided as it moves closer to the trench. This served as the antecedent platform for the formation of Apo Reef. (**C**) Tubbataha Reef is formed by successive reef build-up atop the subsiding Cagayan Ridge

Subsidence rates ranging between 0.7 and 1 mm/year are proposed for Tubbataha Reef. Compared to Apo Reef, vertical movements due to thermal cooling are likely to be more gradual than episodic. These rates represent the difference in subsidence between an actively subsiding region versus a passively subsiding Cagayan Ridge.

Conclusions

The geomorphology of the seafloor around coral reefs reveals the history of sea-level change in a region. The bathymetry around Apo Reef, Mindoro, and Tubbataha Reef North Atoll, Palawan in the Philippines documents the occurrence of submerged terraces that were formed post-LGM. The morphology follows the non-uniform sea-level rise during the last deglaciation, characterized by meltwater pulses and stillstands, resulting in a staircase-like formation of terraces. The sites reveal relative submergence when compared to known records of sea-level change within the West Pacific and the Philippines. Apo Reef experiences tectonic subsidence due to a downbowing lithosphere. Tubbataha Reef experiences thermal subsidence which is attributed to the continuing cooling of an extinct island arc.

Data Availability The datasets generated in the study are available from the corresponding author on reasonable request.

Code availability Not applicable.

Declarations

Ethics approval Not applicable.

Consent to participate Not applicable.

Consent for publication Not applicable.

Competing interests The authors declare no competing interests.

References

Abbey E, Webster JM, Beaman RJ (2011) Geomorphology of submerged reefs on the shelf edge of the Great Barrier Reef: the influence of oscillating Pleistocene sea-levels. Mar Geol 288:61–78. https://doi.org/10.1016/j.margeo.2011.08.006

Abdul NA, Mortlock RA, Wright JD, Fairbanks RG (2016) Younger Dryas sea level and meltwater pulse 1B recorded in Barbados reef crest coral Acropora palmata. Paleoceanography 31:330–344. https://doi.org/10.1002/2015PA002847

Aurelio MA (2000) Shear partitioning in the Philippines: constraints from the Philippine fault and global positioning system data. Isl Arc 9:584–659. https://doi.org/10.1111/j.1440-1738.2000.00304.x

Aurelio MA, Forbes MT, Taguibao KJL, Savella RB, Bacud JA, Franke D, Pubellier M, Savva D, Meressa F, Steuer S, Carranza CD (2014) Middle to Late Cenozoic tectonic events in south and central Palawan (Philippines) and their implications to the evolution of the south-eastern margin of South China Sea: evidence from onshore structural and offshore seismic data. Mar Pet Geol 58:658–673. https://doi.org/10.1016/j.marpetgeo.2013.12.002

Austermann J, Mitrovica JX, Latychev K, Milne GA (2013) Barbados-based estimate of ice volume at Last Glacial Maximum affected by subducted plate. Nat Geosci 6(7):553–557. https://doi.org/10.1038/ngeo1859

Bacabac MMA, Ticzon VS, Fetil JGC, Villanada KDT (2023) Mapping coral reef habitats of Apo Reef Natural Park. Sablayan, Occidental Mindoro. Sci Engg J 16

Bard E, Hamelin B, Arnold M, Montaggioni L, Cabioch G, Faure G, Rougerie F (1996) Deglacial sea-level record from Tahiti corals and the timing of global meltwater discharge. Nature 382:241–244. https://doi.org/10.1038/382241a0

Bastos AC, D'Agostini DP, Silva AE, Menandro PS, Vieira FV, Boni GC, Quaresma VS, Cetto PH (2022) Sedimentological and morphological evidences of meltwater pulse 1B in the Southwestern Atlantic Margin. Mar Geol 450:106850. https://doi.org/10.1016/j.margeo.2022.106850

Beaman RJ, Webster JM, Wust RAJ (2008) New evidence for drowned shelf edge reefs in the Great Barrier Reef, Australia. Mar Geol 247:17–34. https://doi.org/10.1016/j.margeo.2007.08.001

Berdin RD, Siringan FP, Maeda Y (2003) Holocene relative sea-level changes and mangrove response in southwest Bohol, Philippines. J Coast Res 19:304–313

Blanchon P, Medina-Valmaseda A, Hibbert FD (2021) Revised postglacial sea-level rise and meltwater pulses from Barbados. Open Quaternary 1–12. https://doi.org/10.5334/oq.87

Blanchon P, Shaw J (1995) Reef drowning during the last deglaciation: evidence for catastrophic sea-level rise and ice-sheet collapse. Geology 23:4–8. https://doi.org/10.1130/0091-7613(1995)023%3C0004:RDDTLD%3E2.3.CO;2

Brendryen J, Haflidason H, Yokoyama Y, Haaga KA, Hannisdal B (2020) Eurasian ice sheet collapse was a major source of meltwater pulse 1A 14,600 years ago. Nat Geosci 13(5):363–368. https://doi.org/10.1038/s41561-020-0567-4

Calder BR, Mayer LA (2003) Automatic processing of high-rate, high-density multibeam echosounder data. Geochem Geophys Geosyst 4(6). https://doi.org/10.1029/2002GC000486

Chen PF, Olavere EA, Wang CW, Bautista BC, Solidum RU Jr, Liang WT (2015) Seismotectonics of Mindoro, Philippines. Tectonophysics 640:70–79. https://doi.org/10.1016/j.tecto.2014.11.023

Clark PU, Mix AC (2002) Ice sheets and sea level of the Last Glacial Maximum. Quat Sci Rev 21:1–7. https://doi.org/10.1016/S0277-3791(01)00118-4

Clark PU, Tarasov L (2014) Closing the sea level budget at the Last Glacial Maximum. Proc Natl Acad Sci 111(45):15861–15862

Clark PU, McCabe AM, Mix AC, Weaver AJ (2004) Rapid rise of sea level 19,000 years ago and its global implications. Science 304:1141–1144. https://doi.org/10.1126/science.1094449

Conway KW, Barrie JV, Krautter M (2005) Geomorphology of unique reefs on the western Canadian shelf: sponge reefs mapped by multibeam bathymetry. Geo-Marine Letters 25:205–213. https://doi.org/10.1007/s00367-004-0204-z

da Silveira CB, Strenzel GM, Maida M, Araújo TC, Ferreira BP (2020) Multiresolution satellite-derived bathymetry in shallow coral reefs: improving linear algorithms with geographical analysis. J Coastal Res 36(6):1247–1265. https://doi.org/10.2112/JCOASTRES-D-19-00029.1

Davies PJ, Montaggioni LF (1985) Reef growth and sea level: the environmental signature. Antenne Muséum-EPHE

Dechnik B, Webster JM, Davies PJ, Braga JC, Reimer PJ (2015) Holocene "turn-on" and evolution of the Southern Great Barrier Reef: revisiting reef cores from the Capricorn Bunker Group. Mar Geol 363:174–190. https://doi.org/10.1016/j.margeo.2015.02.014

Deschamps P, Durand N, Bard E, Hamelin B, Camoin G, Thomas AL, Henderson GM, Okuno J, Yokoyama Y (2012) Ice-sheet collapse and sea-level rise at the Bølling warming 14,600 years ago. Nature 483:559–564. https://doi.org/10.1038/nature10902

Dickinson WR (2001) Paleoshoreline record of relative Holocene sea levels on Pacific Islands. Earth-Science Rev 55:191–234. https://doi.org/10.1016/S0012-8252(01)00063-0

Dickinson WR (2013) Control of paleoshorelines by trench forebulge uplift. Loyalty Islands Quaternary Res 80(1):125–137. https://doi.org/10.1016/j.yqres.2013.04.007

Dullo WC (2005) Coral growth and reef growth: a brief review. Facies 51:33–48. https://doi.org/10.1007/s10347-005-0060-y

Dygico M, Songco A, White AT, Green SJ (2013) Achieving MPA effectiveness through application of responsive governance incentives in the Tubbataha reefs. Mar Policy 4:87–94. https://doi.org/10.1016/j.marpol.2012.12.031

Fairbanks RG (1989) A 17,000-year glacio-eustatic sea level record: influence of glacial melting rates on the Younger Dryas event and deep-ocean circulation. Nature 342:637–642. https://doi.org/10.1038/342637a0

Fairbanks RG, Charles CD, Wright JD (1992) Origin of global meltwater pulses. In Radiocarbon after four decades: an interdisciplinary perspective (pp. 473-500). Springer, New York, New York, NY

Faure M, Marchadier Y, Rangin C (1989) Pre-Eocene synmetamorphic structure in the Mindoro-Romblon-Palawan area, West Philippines, and implications for the history of Southeast Asia. Tectonics 8:963–979. https://doi.org/10.1029/TC008i005p00963

Franke D, Savva D, Pubellier M, Steuer S, Mouly B, Auxietre JL, Meresse F, Chamot-Rooke N (2014) The final rifting evolution in the South China Sea. Mar Pet Geol 58:704–720. https://doi.org/10.1016/j.marpetgeo.2013.11.020

Fürstenau J, Lindhorst S, Betzler C, Hübscher C (2010) Submerged reef terraces of the Maldives (Indian Ocean). Geo-Marine Lett 30:511–515. https://doi.org/10.1007/s00367-009-0174-2

Glenn-Sullivan EC, Evans I (2001) The effects of time-averaging and taphonomy on the identification of reefal sub-environments using larger foraminifera: Apo Reef, Mindoro, Philippines. Palaios 16:399–408. https://doi.org/10.1669/0883-1351(2001)016%3C0399:TEOTAA%3E2.0.CO;2

Gomes MP, Vital H, Droxler AW (2020) Terraces, reefs, and valleys along the Brazil northeast outer shelf: deglacial sea-level archives? Geo-Marine Lett 40:699–711. https://doi.org/10.1007/s00367-020-00666-4

Gong S, Li H, Siringan FP, Zhao M, Kang S (2017) AMS carbon-14 dating of microbial carbonates in Holocene coral reefs, Western Luzon, Philippines. Quat Int 447:27–34. https://doi.org/10.1016/j.quaint.2017.06.015

Gordon AL, Sprintall J, Ffield A (2011) Regional oceanography of the Philippine Archipelago. Oceanography 24:14–27

Gowan EJ, Zhang X, Khosravi S, Rovere A, Stocchi P, Hughes AL, Gyllencreutz R, Mangerud J, Svendsen J, Lohmann G (2021) A new global ice sheet reconstruction for the past 80 000 years. Nat Commun 12(1):1199. https://doi.org/10.1038/s41467-021-21469-w

Grigg RW, Grossman EE, Earle SA, Gittings SR, Lott D, McDonough J (2002) Drowned reefs and antecedent karst topography, Au'au channel, S.E. Hawaiian Islands Coral Reefs 21:73–82. https://doi.org/10.1007/s00338-001-0203-8

Grossman EE, Fletcher CH (2004) Holocene reef development where wave energy reduces accommodaton space. Kailua Bay, Windward Oahu, Hawaii. J Sediment Res 74(1):49–63. https://doi.org/10.1306/070203740049

Hall R, Ali JR, Anderson CD, Baker SJ (1995) Origin and motion history of the Philippine Sea Plate. Tectonophysics 251(1–4):229–250.v. https://doi.org/10.1016/0040-1951(95)00038-0

Hanebuth T, Stattegger K, Grootes PM (2000) Rapid flooding of the Sunda Shelf: a late-glacial sea-level record. Science 288:1033–1035. https://doi.org/10.1126/science.288.5468.1033

Hanebuth TJJ, Voris HK, Yokoyama Y, Saito Y (2011) Earth-science reviews formation and fate of sedimentary depocentres on Southeast Asia's Sunda Shelf over the past sea-level cycle and biogeographic implications. Earth Sci Rev 104:92–110. https://doi.org/10.1016/j.earscirev.2010.09.006

Harris PT, Heap AD, Marshall JF, Mcculloch M (2008) A new coral reef province in the Gulf of Carpentaria, Australia: colonisation, growth and submergence during the early Holocene. Mar Geol 251:85–97. https://doi.org/10.1016/j.margeo.2008.02.010

Harrison S, Smith DE, Glasser NF (2019) Late Quaternary meltwater pulses and sea level change. J Quaternary Sci 34(1):1–15. https://doi.org/10.1002/jqs.3070

Hayes DE, Lewis SD (1984) A geophysical study of the Manila Trench, Luzon, Philippines: 1. Crustal structure, gravity, and regional tectonic evolution. J Geophys Res Solid Earth 89(B11):9171–9195. https://doi.org/10.1029/JB089iB11p09171

Hongo C, Kayanne H (2009) Holocene coral reef development under windward and leeward locations at Ishigaki Island. Ryukyu Islands, Japan 214(1–4):62–73. https://doi.org/10.1016/j.sedgeo.2008.01.011

Horton BP, Kopp RE, Garner AJ, Hay CC, Khan NS, Roy K, Shaw TA (2018) Mapping sea-level change in time space, and probability. Annu Rev Environ Resour 43:481–521. https://doi.org/10.1146/annurev-environ-102017-025826

Hubbard DK, Gill IP, Burke RB, Morelock J (1997) Holocene reef backstepping—southwestern Puerto Rico shelf. In Proc 8th Int Coral Reef Symp 2:1779–1784

Hurlburt HE, Metzger EJ, Sprintall J, Riedlinger SN, Arnone RA, Shinoda T, Xu X (2011) Circulation in the Philippine Archipelago simulated by 1/12 and 1/25 global HYCOM and EAS NCOM. Oceanography 24(1):28–47

Inoue T, Arai K (2020) New findings on submerged patch reefs and reefal carbonate rocks at water depths of 70–100 m on the insular shelf off Miyako-jima, southern Ryukyus, Japan. Prog Earth Planet Sci 7(1):1–10

Janer DFS, Gabuyo MRP, Carrillo ADV, Co PEY, del Rosario ALB, Morata MJS, Siringan FP et al (2023) Development of Pag-asa Reefs, West Philippine Sea: role of relative sea level change and wave exposure. Philippine J Sci 152(1):291–306

Kan H, Urata K, Nagao M, Hori N, Fujita K, Yokoyama Y, Nakashima Y, Ohashi T, Goto K, Suzuki A (2015) Submerged karst landforms observed by multibeam bathymetric survey in Nagura Bay, Ishigaki Island, southwestern Japan. Geomorphol 229:112–124. https://doi.org/10.1016/j.geomorph.2014.07.032

Kench PS, Ford MR, Bramante JF, Ashton AD, Donnelly JP, Sullivan RM, Toomey MR (2022) Heightened storm activity drives late Holocene reef island formation in the central Pacific Ocean. Global Planet Change 215:103888. https://doi.org/10.1016/j.gloplacha.2022.103888

Kennedy DM, Woodroffe CD (2002) Fringing reef growth and morphology: a review. Earth-Sci Rev 57:255–277. https://doi.org/10.1016/S0012-8252(01)00077-0

Kershaw S, Guo L (2001) Marine notches in coastal cliffs: indicators of relative sea-level change, Perachora Peninsula. Central Greece Mar Geol 179(3–4):213–228. https://doi.org/10.1016/S0025-3227(01)00218-3

Khanna P, Droxler AW, Nittrouer JA, Tunnell JW, Shirley TC (2017) Coralgal reef morphology records punctuated sea-level rise during the last deglaciation /704/106/413 /704/445/215 article. Nat Commun 8. https://doi.org/10.1038/s41467-017-00966-x

Kim CH, Park JW, Lee MH, Park CH (2013) Detailed bathymetry and submarine terraces in the coastal area of the Dokdo Volcano in the Ulleung Basin, the East Sea (Sea of Japan). J Coastal Res 65:523–528. https://doi.org/10.2112/SI65-089.1

Krause DC (1966) Tectonics, marine geology, and bathymetry of the Celebes Sea-Sulu Sea region. Geol Soc Am Bull 77:813–832. https://doi.org/10.1130/0016-7606(1966)77[813:TMGABO]2.0.CO;2

Kudrass, HR, Muller, P, Kreuzer, H, Weiss, W (1990) Volcanic rocks and tertiary carbonates dredged from the Cagayan Ridge and the Southwest Sulu Sea, Philippines. In Rangin, C, Silver, EA, von Breymann, MT, et al., Proc. ODP, Init. Repts (Vol. 124, pp. 93–100). https://doi.org/10.2973/odp.proc.ir.124.106.1990

Lambeck K, Rouby H, Purcell A, Sun Y, Sambridge M (2014) Sea level and global ice volumes from the Last Glacial Maximum to the Holocene. Proc Natl Acad Sci USA 111:15296–15303. https://doi.org/10.1073/pnas.1411762111

Lebrec U, Riera R, Paumard V, O'Leary MJ, Lang SC (2022) Morphology and distribution of submerged palaeoshorelines: insights from the North West Shelf of Australia. Earth Sci Rev 224:103864. https://doi.org/10.1016/j.earscirev.2021.103864

Ledesma MC (2001) Monitoring Tubbataha Reef National Marine Park (TRNMP) and areas along the Cagayan Ridge. Tubbataha Management Office

Li J, Zhang Y, Dong S, Johnston ST (2014) Cretaceous tectonic evolution of South China: a preliminary synthesis. Earth Sci Rev 134:98–136. https://doi.org/10.1016/j.earscirev.2014.03.008

Li T, Chua S, Tan F, Khan NS, Shaw TA, Majewski J, Meltzner AJ, Switzer AD, Wu P, Horton BP (2023) Glacial isostatic adjustment modelling of the mid-Holocene sea-level highstand of Singapore and Southeast Asia. Quaternary Sci Rev 319:108332. https://doi.org/10.1016/j.quascirev.2023.108332

Lighty RG, Macintyre IG, Stuckenrath R (1982) Acropora palmata reef framework: a reliable indicator of sea level in the western Atlantic for the past 10,000 years. Coral Reefs 1:125–130. https://doi.org/10.1007/BF00301694

Lin Y, Hibbert FD, Whitehouse PL, Woodroffe SA, Purcell A, Shennan I, Bradley SL (2021) A reconciled solution of meltwater pulse 1A sources using sea-level fingerprinting. Nat Commun 12(1):2015. https://doi.org/10.1038/s41467-021-21990-y

Linsley BK, Thunell RC (1990) The record of deglaciation in the Sulu Sea: evidence for the Younger Dryas event in the tropical western Pacific. Paleoceanography 5(6):1025–1039. https://doi.org/10.1029/PA005i006p01025

Liu JP, Milliman JD (2004) Reconsidering melt-water pulses 1A and 1B: global impacts of rapid sea-level rise. J Ocean Univ China 3:183–190. https://doi.org/10.1007/s11802-004-0033-8

Liu JP, Milliman JD, Gao S, Cheng P (2004) Holocene development of the Yellow River's subaqueous delta, North Yellow Sea. Mar Geol 209:45–67. https://doi.org/10.1016/j.margeo.2004.06.009

Lutzenkirchen LL, Duce SJ, Bellwood DR (2023) The global biogeography of reef morphology. Global Ecol Biogeogr. https://doi.org/10.1111/geb.13699

Maeda Y, Siringan F (2004) Atlas of Holocene notches and the coral reef terraces of the Philippine Island. Nat Hum Act 8:97–175

Maeda Y, Siringan F, Omura A, Berdin R, Hosono Y, Atsumi S, Nakamura T (2004) Higher-than-present Holocene mean sea levels in Ilocos, Palawan and Samar, Philippines. Quat Int 115–116:15–26. https://doi.org/10.1016/S1040-6182(03)00093-4

Maeda Y, Yokoyama Y, Siringan FP, Quina G (2009) Holocene relative sea-level fluctuations recorded in tidal notches along the Pacific Coast of Northern Luzon, Philippines. J Geogr (chigaku Zasshi) 118:1284–1291. https://doi.org/10.5026/jgeography.118.1284

Mann T, Bender M, Lorscheid T, Stocchi P, Vacchi M, Switzer AD, Rovere A (2019) Holocene sea levels in Southeast Asia, Maldives, India and Sri Lanka: the SEAMIS database. Quaternary Sci Rev 219:112–125. https://doi.org/10.1016/j.quascirev.2019.07.007

Marchadier Y, Rangin C (1990) Polyphase tectonics at the southern tip of the Manila trench, Mindoro-Tablas Islands. Philippines Tectonophys 183(1–4):273–287. https://doi.org/10.1016/0040-1951(90)90421-4

Maxwell KV, Ramos NT, Tsutsumi H, Chou YC, Duan F, Shen CC (2018) Late Quaternary uplift across northwest Luzon Island, Philippines constrained from emergent coral reef terraces. Earth Surf Process Landforms 43:3114–3132. https://doi.org/10.1002/esp.4474

Meltzner AJ, Switzer AD, Horton BP, Ashe E, Qiu Q, Hill DF, Bradlet SL, Kopp RE, Hill EM, Majewski JM, Natawidjaja DH, Suwargadi BW (2017) Half-metre sea-level fluctuations on centennial timescales from mid-Holocene corals of Southeast Asia. Nat Commun 8(1):14387. https://doi.org/10.1038/ncomms14387

Milne GA, Mitrovica JX (2008) Searching for eustasy in deglacial sea-level histories. Quat Sci Rev 27:2292–2302. https://doi.org/10.1016/j.quascirev.2008.08.018

Montaggioni LF (2005) History of Indo-Pacific coral reef systems since the last glaciation: development patterns and controlling factors. Earth Sci Rev 71(1–2):1–75. https://doi.org/10.1016/j.earscirev.2005.01.002

National Mapping and Resource Information Authority (2022) Tide and currents tables 2022. National Mapping and Resource Information Authority, Manila

Neumann AC, Macintyre IG (1985) Reef response to sea level rise: keep-up, catch-up or give-up. Proc Fifth Int Coral Reef Congr 3:105–110

Omura A, Maeda Y, Kawana T, Siringan FP, Berdin RD (2004) U-series dates of Pleistocene corals and their implications to the paleo-sea levels and the vertical displacement in the Central Philippines. Quat Int 115:3–13. https://doi.org/10.1016/S1040-6182(03)00092-2

Ota Y, Chappell J (1999) Holocene sea-level rise and coral reef growth on a tectonically rising coast, Huon Peninsula, Papua New Guinea. Quat Int 55:51–59. https://doi.org/10.1016/S1040-6182(98)00024-X

Pastier AM, Husson L, Pedoja K, Bézos A, Authemayou C, Arias-Ruiz C, Cahyarini SY (2019) Genesis and architecture of sequences of Quaternary coral reef terraces: insights from numerical models. Geochem Geophys Geosyst 20(8):4248–4272. https://doi.org/10.1029/2019GC008239

Peltier WR (2002) On eustatic sea level history: Last Glacial Maximum to Holocene. Quat Sci Rev 21:377–396. https://doi.org/10.1016/S0277-3791(01)00084-1

Perry CT, Smithers SG, Gulliver P, Browne NK (2012) Evidence of very rapid reef accretion and reef growth under high turbidity and terrigenous sedimentation. Geology 40:719–722. https://doi.org/10.1130/G33261.1

Pubellier M, Aurelio M, Sautter B (2018) The life of a marginal basin depicted in a structural map of the South China Sea. Episodes J Int Geosci 41(3):139–142. https://doi.org/10.18814/epiiugs/2018/018014

Pullen JD, Gordon AL, Sprintall J, Lee CM, Alford MH, Doyle JD, May PW (2011) Atmospheric and oceanic processes in the vicinity of an Island Strait. Oceanography 24:112–121. https://doi.org/10.5670/oceanog.2011.08

Ramos NT, Tsutsumi H (2010) Evidence of large prehistoric offshore earthquakes deduced from uplifted Holocene marine terraces in Pangasinan Province, Luzon Island, Philippines. Tectonophysics 495:145–158. https://doi.org/10.1016/j.tecto.2010.08.007

Ramos NT, Tsutsumi H, Perez JS, Bermas PP (2012) Uplifted marine terraces in Davao Oriental Province, Mindanao Island, Philippines and their implications for large prehistoric offshore earthquakes along the Philippine trench. J Asian Earth Sci 45:114–125. https://doi.org/10.1016/j.jseaes.2011.07.028

Rangin C, Silver EA (1991) Neogene tectonic evolution of the Celebes-Sulu basins: new insights from Leg 124 drilling. Proc Sci results ODP Leg 124 Celeb Sulu Seas 124:51–63. https://doi.org/10.2973/odp.proc.sr.124.122.1991

Rangin C, Stephan JF, Blanchet R, Baladad D, Bouysee P, Chen MP, Chotin P, Collot JY, Daniel J, Drouhot JM, Marchadier Y, Marsset B, Pelletier B, Richard MA, Tardy M (1988) Seabeam survey at the southern end of the Manila trench. Transition between subduction and collision processes, offshore Mindoro Island Philippines. Tectonophysics 146(1–4):261–278. https://doi.org/10.1016/0040-1951(88)90095-9

Rangin C, Jolivet L, Pubellier M (1990) A simple model for the tectonic evolution of Southeast Asia and Indonesia region for the past 43 my. Bull de la Société géologique de France v6(6):889–905

Ringor CL, Omura A, Maeda Y (2004) Last Interglacial terraces sea level in southwest changes deduced central from coral reef Philippines U-series sea level history in southwest Bohol during the Last Interglacial or the marine isotope. Quat Res (Daiyonki-Kenkyu) 43(6):401–406. https://doi.org/10.4116/jaqua.43.401

Rovere A, Khanna P, Bianchi CN, Droxler AW, Morri C, Naar DF (2018) Submerged reef terraces in the Maldivian Archipelago (Indian Ocean). Geomorphology 317:218–232. https://doi.org/10.1016/j.geomorph.2018.05.026

Salas-Saavedra M, Dechnik B, Webb GE, Webster JM, Zhao JX, Nothdurft LD, Clark TR, Graham T, Duce S (2018) Holocene reef growth over irregular Pleistocene karst confirms major influence of hydrodynamic factors on Holocene reef development. Quaternary Sci Rev 180:157–176. https://doi.org/10.1016/j.quascirev.2017.11.034

Saldivar-Sali A, Oesterle HG, Brownlee DN (1981) The geology of offshore northwest Palawan, Philippines-1. Oil and Gas J 119–128

Sarewitz DR, Karig DE (1986) Processes of allochthonous terrane evolution, Mindoro Island, Philippines. Tectonics 5:525–552. https://doi.org/10.1029/TC005i004p00525

Shaw TA, Li T, Ng T, Cahill N, Chua S, Majewski JM, Horton BP et al (2023) Deglacial perspectives of future sea level for Singapore. Commun Earth Environ 4(1):204. https://doi.org/10.1038/s43247-023-00868-5

Shen CC, Siringan FP, Lin K, Dai CF, Gong SY (2010) Sea-level rise and coral-reef development of Northwestern Luzon since 9.9 ka. Palaeogeogr Palaeoclimatol Palaeoecol 292:465–473. https://doi.org/10.1016/j.palaeo.2010.04.007

Siringan FP, Shen CC, Lin K, Abigania MIT, Gong SY (2016) Coral-based Holocene sea level of Paraoir, western Luzon, Philippines. J Asian Earth Sci 123:61–66. https://doi.org/10.1016/j.jseaes.2016.03.022

Smith SV, Buddemeier RW (1992) Global change and coral reef ecosystems. Annu Rev Ecol Syst 23(1):89–118. https://doi.org/10.1146/annurev.es.23.110192.000513

Steuer S, Franke D, Meresse F, Savva D, Pubellier M, Aurelio AJL, M, (2013) Time constraints on the evolution of southern Palawan Island, Philippines from onshore and offshore correlation of Miocene limestones. J Asian Earth Sci 76:412–427

Stoddart DR (1969) Ecology and morphology of recent coral reefs. Biol Rev 44(4):433–498. https://doi.org/10.1111/j.1469-185X.1969.tb00609.x

Stoddart DR (1990) Coral reefs and islands and predicted sea-level rise. Prog Phys Geogr 14(4):521–536. https://doi.org/10.1177/030913339001400405

Storlazzi CD, Logan JB, Field ME (2003) Quantitative morphology of a fringing reef tract from high-resolution laser bathymetry: Southern Molokai. Hawaii Geol Soc Am Bull 115(11):1344–1355. https://doi.org/10.1130/B25200.1

Tian SY, Yasuhara M, Hong Y, Huang HHM, Iwatani H, Chiu WTR, Mamo B, Okahashi H, Rasmussen TL (2020) Deglacial-Holocene Svalbard paleoceanography and evidence of meltwater pulse 1B. Quaternary Sci Rev 233:106237. https://doi.org/10.1016/j.quascirev.2020.106237

Tibor G, Niemi TM, Ben-Avraham Z, Al-Zoubi A, Sade RA, Hall JK, Hartman G, Akawi E, Abueladas A, Al-Ruzouq R (2010) Active tectonic morphology and submarine deformation of the northern Gulf of Eilat/Aqaba from analyses of multibeam data. Geo-Marine Lett 30:561–573. https://doi.org/10.1007/s00367-010-0194-y

Varzi AG, Fallati L, Savini A, Bracchi VA, Bazzicalupo P, Rosso A, Sanfilippo R, Bertolino M, Muzzupappa M, Basso D (2023). Geomorphology of coralligenous reefs offshore southeastern Sicily (Ionian Sea). J Maps 1–13. https://doi.org/10.1080/17445647.2022.2161963

Vieira FV, Bastos AC, Quaresma VS (2023). Submerged reef and inter-reef morphology in the Western South Atlantic, Abrolhos Shelf (Brazil). Geomorphology 108917. https://doi.org/10.1016/j.geomorph.2023.108917

Waelbroeck C, Labeyrie L, Michel E, Duplessy JC, Mcmanus JF, Lambeck K, Balbon E, Labracherie M (2002) Sea-level and deep water temperature changes derived from benthic foraminifera isotopic records. Quat Sci Rev 21(1–3):295–305. https://doi.org/10.1016/S0277-3791(01)00101-9

Wang J, Qi Y, Jones IS (2006) An analysis of the characteristics of chlorophyll in the Sulu Sea. J Mar Syst 59(1–2):111–119. https://doi.org/10.1016/j.jmarsys.2005.09.004

Weaver AJ, Saenko OA, Clark PU, Mitrovica JX (2003) Meltwater pulse 1A from Antarctica as a trigger of the Bølling-Allerød warm interval. Science 299:1709–1713. https://doi.org/10.1126/science.1081002

Webster JM, Braga JC, Humblet M, Potts DC, Iryu Y, Yokoyama Y, Fujita K, Bourillot R, Esat TM, Fallo S et al (2018) Response of the Great Barrier Reef to sea-level and environmental changes over the past 30,000 years. Nat Geosci 11:426–432. https://doi.org/10.1038/s41561-018-0127-3

White AT, Palaganas VP (1991) Philippine Tubbataha Reef National Marine Park: status, management issues, and proposed plan. Environ Conserv 18:148–157. https://doi.org/10.1017/S0376892900021731

Wood R (1999) Reef evolution. Oxford University Press

Woodroffe CD (2008) Reef-island topography and the vulnerability of atolls to sea-level rise. Global Planet Change 62(1–2):77–96. https://doi.org/10.1016/j.gloplacha.2007.11.001

Woodroffe CD, Webster JM (2014) Coral reefs and sea-level change. Mar Geol 352:248–267. https://doi.org/10.1016/j.margeo.2013.12.006

Wyrtki K (1961) Physical oceanography of the Southeast Asian waters, vol 2. University of California, Scripps Institution of Oceanography

Yokoyama Y, Lambeck K, De Deckker P, Johnston P, Fifield LK (2001) Timing of the Last Glacial Maximum from observed sea-level minima. Nature 412(6842):99–99. https://doi.org/10.1038/35083629

Zacher W, (1981) Geology and morphology of Apo Reef: Proceedings of the Fourth Coral Reef Symposium. Proceedings Fourth Coral Reef Symp 596

Zamoras LR, Matsuoka A (2004) Accretion and postaccretion tectonics of the Calamian Islands, North Palawan block. Philippines Island Arc 13(4):506–519. https://doi.org/10.1111/j.1440-1738.2004.00443.x

Zecchin M, Ceramicola S, Lodolo E, Casalbore D, Chiocci FL (2015) Episodic, rapid sea-level rises on the central Mediterranean shelves after the Last Glacial Maximum: a review. Marine Geo 369:212–223. https://doi.org/10.1016/j.margeo.2015.09.002